ISPRS Journal of Photogrammetry and Remote Sensing 227 (2025) 84–98

Contents lists available at ScienceDirect

ISPRS Journal of Photogrammetry and Remote Sensing

journal homepage: www.elsevier.com/locate/isprsjprs

A weight-adaptive updated method for grasshopper habitat mapping at the national scale using remote sensing: Combined with spatial heterogeneity and landscape

Jing Guo [a,b], Wenjiang Huang [a,b,*], Yingying Dong [a,b,*], Kejian Lin [c], Fangzheng Yue [d,e], Yanmin Shan [f], Huan Liu [f], Zhuoqing Hao [a,b], Ning Wang [c], Xiaolong Ding [c]

[a] State Key Laboratory of Remote Sensing and Digital Earth, Aerospace Information Research Institute, Chinese Academy of Sciences, Beijing 100101, China
[b] University of Chinese Academy of Sciences, Beijing 100049, China
[c] Key Laboratory of Biohazard Monitoring and Green Prevention and Control in Artificial Grassland, Ministry of Agriculture and Rural Affairs, Institute of Grassland Research, Chinese Academy of Agricultural Sciences, Hohhot 010010 Inner Mongolia, China
[d] Center for Biological Disaster Prevention and Control, National Forestry and Grassland Administration, Shenyang 110034, China
[e] Key Laboratory of National Forestry and Grassland Administration on Forest and Grassland Pest Monitoring and Warning, Shenyang 110034, China
[f] Inner Mongolia Forestry and Grassland Pest Control and Quarantine Station, Hohhot 010000, China

ARTICLE INFO

Keywords:
Grasshopper
Landscape
Spatial heterogeneity
Habitat monitoring
Remote sensing
Pest

ABSTRACT

Grasshoppers pose a significant threat to agriculture and animal husbandry by causing grassland degradation and desertification, which further increase the frequency and severity of grasshopper outbreaks. Therefore, implementing scientific control measures to maintain grasshopper populations within reasonable ecological thresholds is essential for the sustainable development of grassland ecosystems. Understanding the mechanisms underlying the interactions between grasshoppers, host plants, and environmental factors and monitoring suitable habitats is critical for effective grasshopper prevention and control. However, the relative weights of these environmental factors vary depending on the grasshopper species and regional environment. This study focused on the occurrence of seven dominant grasshopper species in China's grasslands. Based on the developmental mechanisms of grasshoppers, representative monitoring indicators of habitats were identified using difference testing, correlation analysis, and importance evaluation. Subsequently, the spatiotemporal patterns and hotspots of grasshopper occurrence were analyzed using historical occurrence data from 2019 to 2023. Finally, considering the landscape and spatial heterogeneity, we developed a large-scale habitat monitoring model with weight-adaptive updating. These results indicated that meteorological conditions significantly influenced the occurrence of *Oedaleus* species. Terrain factors are crucial for determining the distribution of grasshoppers on the Tibetan Plateau, particularly *Chorthippus dubius* and *Locusta migratoria tibetensis*. Soil factors have the greatest influence on the distribution of *Dasyhippus barbipes* in Hulunbuir and *Oxya chinensis* in Heilongjiang. Furthermore, the occurrence of grasshoppers exhibited a significant spatial autocorrelation with hotspot areas primarily located in eastern Inner Mongolia, Qinghai, and Xinjiang. The habitat monitoring results showed that models incorporating both landscape and spatial heterogeneity outperformed models that considered only one of these factors. The most suitable areas are primarily located in the western and northern regions of the Kerqin Grassland, northern and eastern parts of Xilingol, the western region of Hulunbuir, the northern and western parts of Xinjiang, the southwestern region of Gansu, and northwestern parts of Tibet. These findings provide

Abbreviations: AIC, Akaike Information Criterion; AREA, Patch Area; DD, Degree day; EMinT, Minimum temperature during the egg stage; CIRCLE, Related Circumscribing Circle; CL-GWLR, Landscape based Geographically Weighted Logistic Regression in China; CONTIG, Contiguity Index; EMinST, Minimum soil temperature during the egg stage; EP, Total precipitation during the egg period; EST, Mean Soil temperature during the egg stage; FRAC, Fractal Dimension Index; FVC, Fractional Vegetation Cover; GSNI, Gansu Province, Shaanxi Province, Ningxia Hui Autonomous Region, and the central-western regions of Inner Mongolia Autonomous Region; GWLR, Geographically Weighted Logistic Regression; GWR, Geographically Weighted Regression; GYRATE, Radius of Gyration; HAG, Hotspot area of grasshopper; HJLK, Hebei Province, Jilin Province, Liaoning Province, and the Kerqin Grassland; HL, Hulunbuir City; HLJ, Heilongjiang province; KDE, Kernel Density Estimation.

* Corresponding authors at: State Key Laboratory of Remote Sensing and Digital Earth, Aerospace Information Research Institute, Chinese Academy of Sciences. Beijing 100101, China.
E-mail addresses: guojing211@mails.ucas.ac.cn (J. Guo), huangwj@aircas.ac.cn (W. Huang), dongyy@aircas.ac.cn (Y. Dong).

https://doi.org/10.1016/j.isprsjprs.2025.05.033
Received 4 December 2024; Received in revised form 5 May 2025; Accepted 30 May 2025
Available online 11 June 2025

crucial support for the scientific control of grasshoppers and contribute significantly to the sustainable development of agriculture and animal husbandry.

1. Introduction

Grasslands are critical components of terrestrial ecosystems and play vital roles in water conservation, soil preservation, and biodiversity protection (Carlier et al., 2009; Bengtsson et al., 2019; Hu et al., 2024). However, in recent years, grassland ecosystems have been damaged by harmful pests, climate change, and overgrazing, leading to significant ecological and environmental challenges, such as soil erosion and pasture degradation (Neke and Du Plessis, 2004). In turn, pasture degradation increases the prevalence of harmful organisms and results in more frequent pest outbreaks. These threats include pests, rodents, plant diseases, and toxic weeds (Kang et al., 2007), with insect pests, such as grasshoppers, *Gynaephora qinghaiensis*, and leaf beetles, posing the most severe constraints on animal husbandry. Grasshoppers are the most destructive pests globally, occurring across all continents except Antarctica and the outbreaks of grasshoppers affect an estimated 850 million people (Chen, 2008). Grasshoppers are widely distributed across the grasslands of 13 provinces and autonomous regions in China, including Inner Mongolia, Xinjiang, Qinghai, and Tibet. (Fan et al., 2015). Each year, grasshoppers affect approximately 40 million hectares of grasslands, causing significant economic losses and ecological damage to grassland ecosystems. Current grasshopper monitoring methods rely predominantly on manual surveys conducted at specific "points." Although these surveys can achieve high accuracy in localized areas, they are inadequate for large-scale prevention and control. The total area of grasslands in China reaches 13.2 billion mu, accounting for 22 % of the country's total land area. Conventional ground survey methods not only require substantial temporal and human resources but are fundamentally insufficient to support precision monitoring across such extensive spatial grassland areas. Satellite remote sensing technology can provide large-scale information, which enables systematic habitat monitoring at ecologically meaningful scales. Moreover, variation in the dominant grasshopper species and the relative importance of influencing factors across different regions (Guo et al., 2006) add complexity to the management and control of these pests. With the development of remote-sensing technology, the integration of multisource data has enabled the acquisition of continuous spatiotemporal information. Therefore, the researchers can calculate the relative importance of influencing factors across different regions (Tappan et al., 1991; Latchininsky and Sivanpillai, 2010; Waldner et al., 2015; Piou et al., 2023). Furthermore, the habitats of grasshoppers change over time and space. Multi-source satellite net can achieve a global revisit cycle of 1–2 days, allowing for dynamic monitoring using high temporal and spatial resolution satellites, which can effectively capture the changing processes of habitats and provide strong support for the precise prevention and control of grasshoppers.

Grasshopper occurrence is closely linked to environmental conditions; therefore, understanding the interaction between grasshoppers, host plants, and their environments is essential for the precise management of grasshopper populations. Several studies have explored the relationship between specific grasshopper species and habitat factors. For example, precipitation and land use have been identified as key drivers of grasshopper outbreaks in eastern Australia (Veran et al., 2015). Similarly, precipitation, temperature, vegetation coverage, and soil moisture are critical habitat factors influencing desert locusts (Wang et al., 2021). While previous studies have significantly contributed to the understanding of the relationship between grasshopper outbreaks and environmental factors, the relative weights of these factors vary depending on the grasshopper species and environment. Therefore, it is critical to analyze the mechanisms between dominant grasshopper species and habitat factors, identify appropriate monitoring indicators, and establish a comprehensive large-scale monitoring system.

Recently, several researchers have constructed grasshopper monitoring and early warning systems based on the relationship between grasshopper populations and habitat factors in localized grassland areas. For example, Geng et al. (2022) constructed a habitat monitoring model for *Locusta migratoria manilensis* at the landscape scale, achieving a monitoring accuracy of 88 %. Similarly, Kistner-Thomas et al. (2021) developed a regression model to predict grasshopper density by incorporating 72 environmental factors, while accounting for region-specific conditions and landscape heterogeneity, demonstrating high predictive accuracy. Du et al. (2022) used MaxEnt to build a habitat monitoring model for grasshoppers in the Hulunbuir grasslands by coupling multiple factors. The model demonstrated good performance, with accuracies ranging from 89.7 % to 97.3 % over several years. Although these studies achieved high accuracy in localized regions, the weight of the influencing factors for grasshopper populations varies. Models with fixed weights, although effective in specific areas, may not be suitable for large-scale applications because of the variability in habitat factors across broader regions. Therefore, under complex environmental conditions, it is essential to develop a habitat monitoring model that dynamically adjusts the habitat factor weights. This will facilitate more accurate monitoring, enabling a more effective response to the evolving environmental conditions that influence grasshopper occurrence.

In this study, we integrated the growth and development mechanisms of grasshoppers, focusing on seven dominant grasshopper species in occurrence regions across China. The objectives of this study were as follows: 1) Construction of habitat indicator system. Based on the multisource data—including MODIS products (MOD11A1 land surface temperature; MOD13A2 vegetation indices), ERA5-Land reanalysis data (hourly 2 m air temperature, soil temperature at 0–7 cm depth, and precipitation), and SMAP L4 surface soil moisture, gain the environmental factors across four categories (meteorological, vegetation, soil, and topographic) that influence grasshopper growth and development. Then, leveraging these remote sensing products and combined with landscape habitat variables, construct representative monitoring indicators for dominant grasshopper species in each subregion by using differentiation tests, correlation analysis, and importance tests. 2) Analysis of the spatial pattern of grasshoppers. Evaluating the global and local spatial autocorrelation patterns of grasshopper occurrence and identifying hotspot area of grasshopper (HAG) occurrence from 2019 to 2023 using historical data. 3) Construction of a large-scale monitoring model. Based on the monitoring indicators derived from multi-source remote sensing data, we aim to develop a large-scale monitoring model for grasshopper habitats. The findings of this study provide scientific and methodological support for the environmentally sustainable and precise control of grasshoppers, with significant implications for the restoration and sustainable development of grassland ecosystems.

2. Materials and methods

2.1. Study area

Based on historical grasshopper occurrence data provided by the National Forestry and Grassland Administration, the research was conducted across nine ecological regions: GSNI (Gansu Province, Shaanxi Province, Ningxia Hui Autonomous Region, and the central-western regions of Inner Mongolia Autonomous Region), HJLK (Hebei Province, Jilin Province, Liaoning Province, and the Kerqin Grassland, including Chifeng City, Tongliao City, and Hinggan League), HL (Hulunbuir City in Inner Mongolia Autonomous Region), QH (Qinghai Province), SX (Shanxi Province), XC (Tibet Autonomous Region and

Sichuan Province), XJ (Xinjiang Uygur Autonomous Region), and XW (Xilingol League and Ulanqab City in Inner Mongolia Autonomous Region). The dominant grasshopper species in each region were investigated based on historical occurrence data, focusing on seven of the most harmful species: *Oedaleus decorus asiaticus, Dasyhippus barbipes, Calliptamus italicus, Chorthippus dubius, Locusta migratoria tibetensis, Oedaleus infernalis,* and *Oxya chinensis*. The distribution of these ecological regions and their associated dominant grasshopper species are illustrated in Fig. 1.

2.2. Data acquisition and processing

2.2.1. Satellite data

The MODIS products MOD11A1 and MOD13A2 covering the period from 2018 to 2023 were used to obtain land surface temperature (LST) and normalized difference vegetation indices. The LST data included the mean and minimum LST with a temporal resolution of 1 day. Normalized difference vegetation index data were used to calculate the fractional vegetation cover (FVC) with a temporal resolution of 16 days.

2.2.2. Meteorological data

The meteorological data used in this study, spanning the period of 2018 to 2023, included the ERA5_LAND dataset, which provides hourly air temperature (band: temperature_2m), soil temperature (band: soil_temperature_level_1), and precipitation data (band: total_precipitation_sum). The soil temperature and precipitation data had a temporal resolution of 1 day and a spatial resolution of 9 km. Additionally, soil moisture active passive (SMAP) data (band: sm_surface) were sourced from the National Aeronautics and Space Administration, offering a spatial resolution of 9 km and including both mean and minimum soil temperatures.

2.2.3. Soil and topography data

Soil nitrogen, soil pH, soil clay, and topography (elevation, aspect, and slope) data showed little change over the study period. Consequently, we hypothesized that these conditions would remain relatively stable. Soil nitrogen (5–15 cm), pH (5–15 cm), and clay (5–15 cm) data were acquired from 250 m soil grids.

All satellite, meteorological, soil, and topographic data were downloaded and calculated using Google Earth Engine. After preprocessing, which involved mosaicking, masking, and reprojection, all data were resampled to a spatial resolution of 1 km.

2.2.4. Landscape data

Vegetation type was used as a baseline to analyze the landscape characteristics and their influence on grasshopper populations. The vegetation data were sourced from the Editorial Committee of China Vegetation Map, Chinese Academy of Sciences which was updated in 2019, with a resolution of 1:1,000,000. (Vegetation Map of the People's Republic of China (1:1000000), Plant Data Center of Chinese Academy of Sciences, https://doi.org/10.12282/plantdata.0155, CSTR:34735.11.PLANTDATA.0155). The study area encompassed three mega vegetation groups: grasslands, shrublands, and meadows, along with 10 vegetation subcategories, totaling 223 distinct vegetation types, which served as the basis for analysis. Based on recent investigations, the vegetation type in the study areas has remained relatively stable over the past few years; therefore, vegetation type was treated as a static factor in this study.

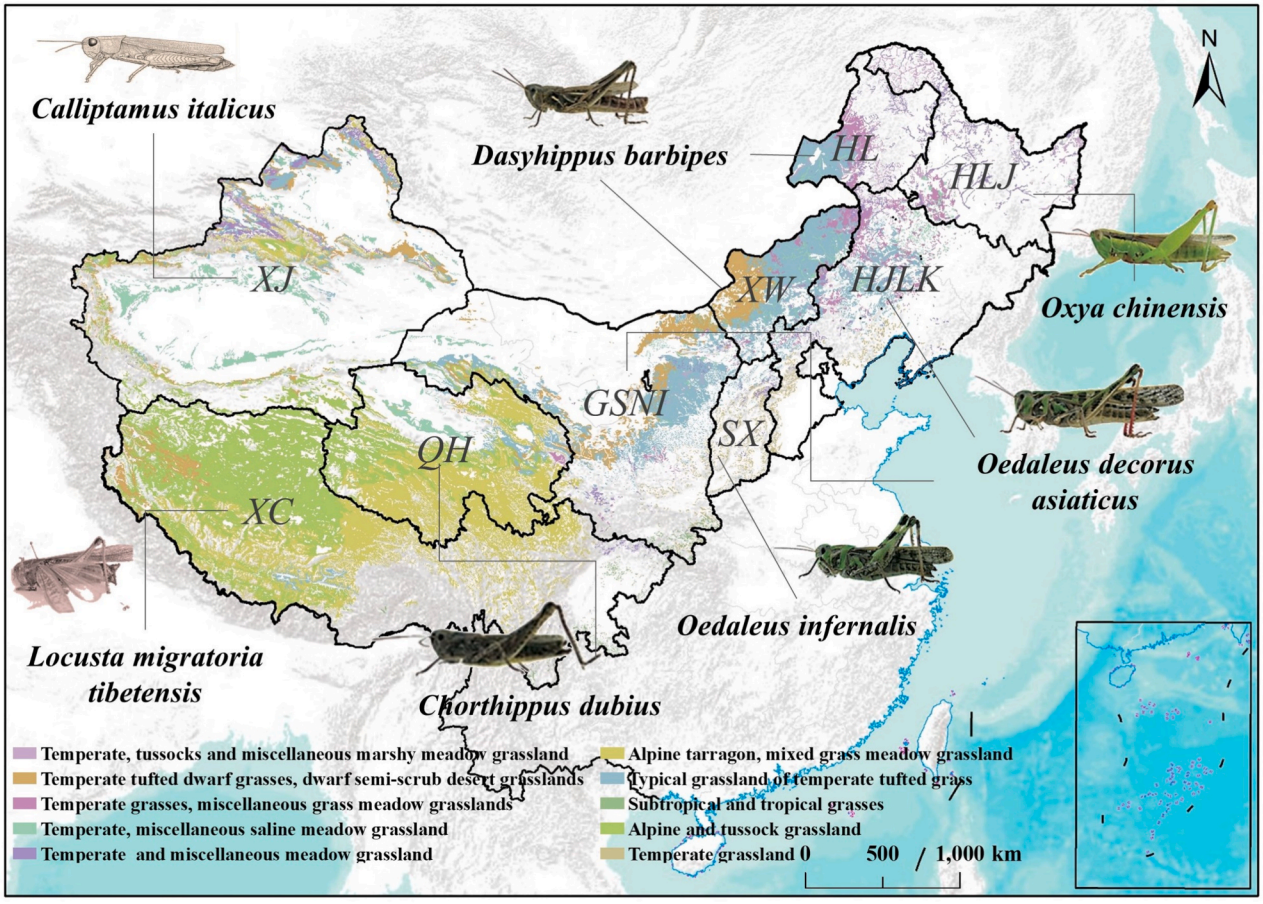

Fig. 1. Distribution of grasshopper distribution areas and dominant species across China. The base map is from the National Standard Vector Map (GS (2023)2767).

2.3. Field survey

Grasshopper occurrence data from 2019 to 2021 (excluding the XW region) were obtained from the Center for Biological Disaster Prevention and Control of the National Forestry and Grassland Administration. This dataset, derived from annual field surveys, was provided as areal data at the farmland level and encompassed all grasshopper-affected areas in China, including both frequently and sporadically occurrence regions. Random sampling points were generated within each pasture according to the reported area of grasshopper occurrence. National grasshopper data for 2022–2023 and data for the XW region for 2019–2023 were collected through a census conducted across each farmland in China and field surveys in XW, respectively. A regional survey methodology adhering to the agricultural industry standards of the People's Republic of China (NY/T 1578-2007: Rules for Investigating Locality and Grasshopper in Grassland), was employed to investigate the occurrence of grasshoppers. A multipoint survey was designed to cover all natural geomorphic units at the farmland level, including areas with regular occurrence, occasional occurrence, and non-occurrence. Sampling plots were set at an average interval of at least 10 km, with each plot measuring 1 km × 1 km to ensure consistency with the spatial resolution of the habitat factor data. Within each plot, a five-point sampling method was employed using subplots measuring 1 m × 1 m to collect detailed data, including geographical coordinates, grasshopper population density, and species composition. Following this methodology, field surveys were conducted annually from May to August during the nymph stage of grasshoppers.

Non-occurrence points in China from 2019 to 2021 (excluding the XW region) were generated using a pseudo-random number generator in regions where no grasshopper occurrences had been recorded by the Center for Biological Disaster Prevention and Control over the past three years (Orchard et al., 1980; Impagliazzo et al., 1989; Bhattacharjee and Das, 2022). In the XW region, absence data from 2019 to 2021 were acquired through standardized farmland field surveys, while 2022–2023 national non-occurrence records were compiled from the National Grassland Pest Census. All surveys strictly adhered to the NY/T 1578-2007 technical protocols. Absence locations were operationally defined as sampling plots with no grasshopper populations during the survey period.

In total, 4,060 grasshopper occurrence points and 3,533 non-occurrence points were collected and used in the subsequent analyses.

2.4. Methodology for weight-adaptive mapping of grasshopper habitats

This study focused on seven dominant grasshopper species in grasshopper-affected provinces across China. Based on the growth, development, and epidemiological mechanisms of grasshoppers, the degree day (DD) model (Naves and de Sousa, 2009) was employed to estimate the growth and development periods of dominant species across different regions, providing a temporal framework for selecting relevant habitat factors. A comprehensive set of 30 habitat monitoring indicators, including meteorological, vegetation, topographic, soil, and ecological factors, were considered for their influence on grasshopper growth and development. Representative habitat indicator systems were identified using differentiation tests, correlation analyses, and importance tests. Subsequently, the global Moran's I index was employed to examine the global spatial autocorrelation of grasshopper occurrence using historical occurrence data from 2019 to 2023. Hotspot analysis and kernel density estimation were then applied to identify localized HAGs. Finally, a large-scale Landscape Geographically Weighted Logistic Regression model in China (CL-GWLR) for grasshopper habitat monitoring that accounted for landscape and spatial heterogeneity was developed using a geographically weighted logistic regression model (GWLR). The performance of the model was compared with that of traditional ordinary least squares (OLS) regression and GWLR, which did not consider landscape factors. The technical framework of this study is illustrated in Fig. 2.

2.4.1. Construction of a grasshopper monitoring indicator system

The distribution of grasshoppers is influenced by the combined effects of meteorological conditions, vegetation, soil, topography, and the ecological environment (Guo et al., 2024), with each factor exerting mutual influence and interdependence on other factors. For instance, temperature plays a critical role in grasshopper development (Hao and Kang, 2004), whereas vegetation affects grasshopper feeding behavior and egg-laying patterns (Mulkern, 1967; Li et al., 2024). Soil moisture affects the survival rate of grasshopper eggs (Mukerji and Gage, 1978), and altitude can influence their distribution by modulating temperature conditions (Leksono et al., 2020). However, the impact of these factors on grasshoppers varies geographically (Karpakakunjaram et al., 2002), and responses to habitat factors differ among species (Bidau et al., 2012). As a result, monitoring indicator systems for the dominant grasshopper species vary. A comprehensive understanding of the mechanisms underlying the interactions between grasshoppers and their environments is essential for explaining and predicting outbreak processes. Therefore, in this study, we selected representative remote sensing monitoring indicators for grasshoppers from 30 habitat factors (Table S1) spanning five categories: meteorology, vegetation, soil, topography, and ecology. These indicators were used to establish a habitat monitoring system for seven grasshopper species across nine regions.

The grasshopper life cycle is divided into three stages: egg, nymph, and adult (Vennard et al., 1998). During each stage, temperature is the primary factor influencing grasshopper growth and development (Yu et al., 2009). Grasshoppers must reach an initial temperature and accumulate a defined amount of heat to transition to the next stage; otherwise, they enter a state of diapause. To accurately define the temporal scope of habitat factors, we integrated the growth mechanisms of grasshoppers with the DD model to determine the developmental periods across different regions (Jin and Wu,1978; Liu et al., 1997; Ji et al., 1991; Qiu et al., 2004; WumaErbieke, 2007; Hui, 2013; Ren et al., 2016; Ji and Ma,2015). Not all of the 24 environmental factors considered had a significant effect on grasshopper occurrence. To identify factors with significant effects, we conducted a difference test on 24 environmental factors and excluded those that did not show a significant influence ($p > 0.05$) (Kennedy-Shaffer, 2019). Statistical methods were selected based on the distribution characteristics of the factors: t-tests for normally distributed variables (García-Pérez, 2006:), Wilcoxon–Mann–Whitney non-parametric tests for non-normally distributed variables (Kühnast and Neuhäuser, 2008), and chi-square tests for categorical variables (Vierra et al., 2023). To avoid strong correlations between the variables, Spearman's correlation analysis was conducted on factors with significant differences. During the variable selection process, the random forest method was employed to assess the importance of the indicators, and factors with correlations exceeding 0.8 and lower importance scores were excluded (Xu et al., 2019).

Given the significant role of vegetation type in grasshopper feeding and habitat preference, vegetation type was used as a baseline to examine how landscape characteristics influence grasshopper occurrence. The landscape area, edge metrics, and shape indices effectively represent the habitat characteristics and complexity of regional landscapes. Consequently, three landscape areas and edge metrics along with four shape indices were selected to construct the monitoring indicator system. These factors were calculated using Fragstats 4.2 software (http://www.umass.edu/landeco/research/fragstats/fragstats.html). Multiple occurrence and non-occurrence points may exist within a single patch. Therefore, testing methods for local variables may not be applicable. We employed correlation analysis and importance tests to optimize landscape variables. First, correlation analysis was performed using the seven landscape factors to explore significant correlations between these variables. Importance tests were used to identify the important factors. Factors that exhibited high correlations ($R > 0.8$) and

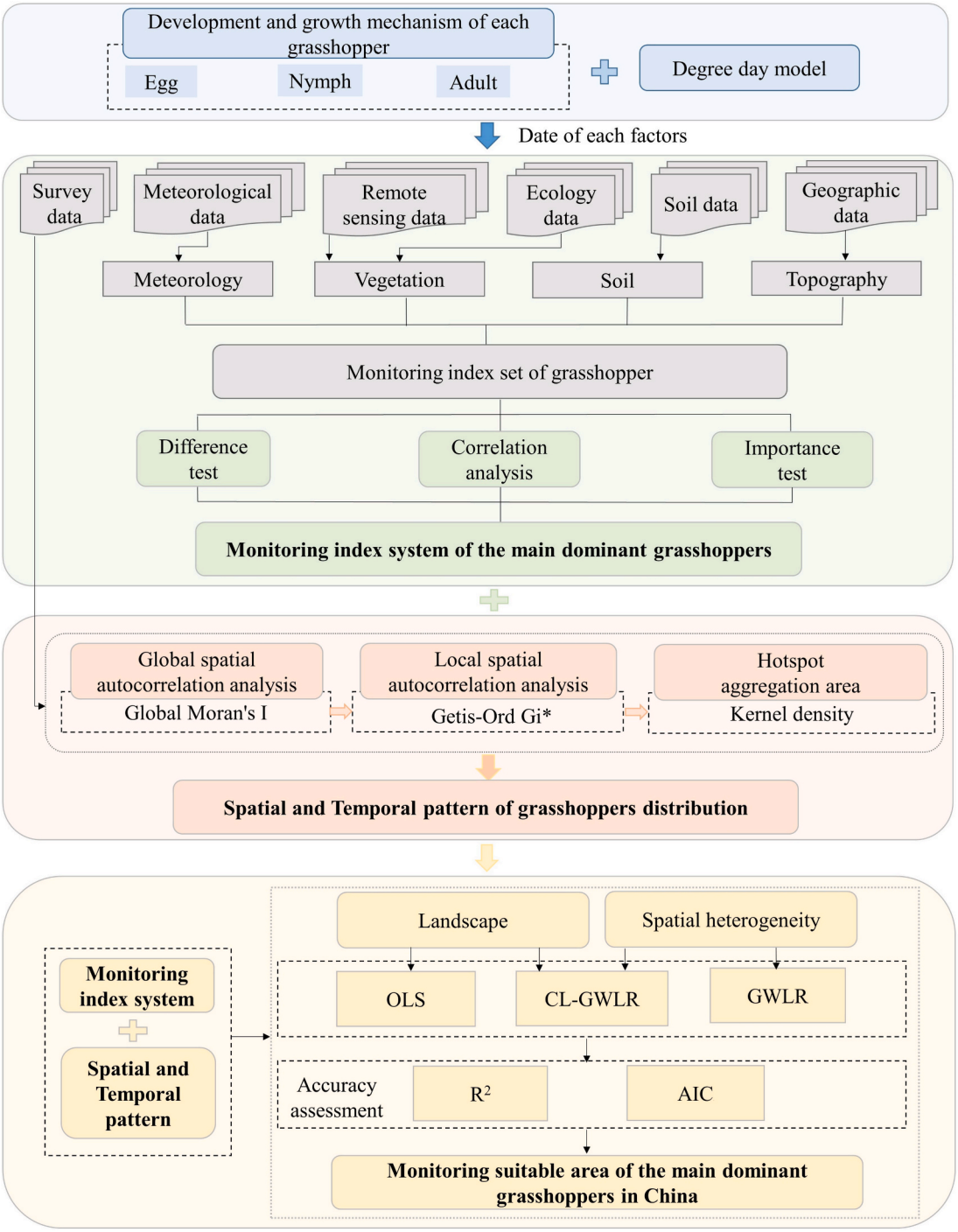

Fig. 2. Flowchart of the study.

had lower importance were excluded.

2.4.2. Spatial and temporal pattern analysis for dominant grasshopper species

The distribution of grasshoppers in the prairie exhibits distinct spatial patterns (Badenhausser et al., 2012; Gauffre et al., 2015). Thus, we investigated the spatiotemporal distribution patterns of HAGs. To quantify spatial autocorrelation, Moran's index (Moran's I), was employed. A Moran's I value greater than zero indicates a positive spatial correlation, with higher values reflecting stronger spatial clustering. Conversely, Moran's I less than 0 indicates a negative spatial correlation, with smaller values indicating greater spatial heterogeneity. A Moran's I of zero suggests a random spatial pattern with no significant correlation (Assuncao and Reis, 1999). To explore the spatial characteristics of grasshopper distributions, the global spatial autocorrelation of grasshopper occurrence was assessed using the Global Moran's Index. Based on historical grasshopper occurrence points, local spatial autocorrelation was analyzed using Getis-Ord Gi* hotspot analysis. Significant hotspots ($z > 1.65$ and $p < 0.05$) were identified using z-scores and p-values, providing a foundation for subsequent modeling (Ghodousi et al., 2020).

Kernel density estimation (KDE) was employed to calculate the density of the points surrounding each output raster cell (Mohaymany et al., 2013). This method provides a clear and intuitive visualization of

HAGs based on historical occurrence data. By applying KDE to significant hotspots, deeper insights into the spatial characteristics of grasshopper occurrence were obtained. KDE is one of the most widely used nonparametric estimation methods in spatial analysis. This method is typically defined as follows: Let S1, …, and Sn be a set of independent samples drawn from a population with a density function f. The estimation of the f value at point s is denoted by $f(s)$ and is calculated using the following estimation formula:

$$f(s) = \sum_{i=1}^{n} \frac{k}{\pi r^2}\left(\frac{d_{is}}{r}\right) \tag{2-1}$$

where n is the sample size, d_{is} is the distance between points i and location s, k is the ratio of d_{is}, and r is the bandwidth determined by the adaptive bandwidth method.

To further analyze the overall spatial distribution and spatiotemporal variation characteristics of grasshoppers, the Standard Deviation Ellipse (SDE) method was employed (Huang et al., 2022). This approach reveals the spatiotemporal migration patterns of grasshoppers by examining changes in the centroid of the SDE over time. These analyses provided valuable insights into the spatiotemporal dynamics of grasshopper populations.

2.4.3. Habitat monitoring model with landscape and spatial heterogeneity

Habitat factors influencing grasshopper development exhibit significant regional variation, and the weight of these factors varies across regions (Ni et al., 2003; Humphreys et al., 2022). Additionally, grasshoppers are influenced not only by local habitat factors but also by surrounding ecological characteristics. Landscape factors, such as landscape type and the number of patches within the same landscape type, can substantially influence species distribution (Steck et al., 2007; Geng et al., 2022). Despite this, many studies on grasshoppers have neglected the effects of surrounding landscape features, limiting the accuracy of habitat mapping models. Models that fail to account for landscape and spatial heterogeneity do not comprehensively represent grasshopper habitat dynamics.

Building on the monitoring indicators system established in Section 2.4.1, we developed a model that integrates Logistic Regression (LR) and Geographically Weighted Regression (GWR). LR is a generalized linear regression approach that estimates the probability of an event based on a given set of independent variables and is particularly effective for binary variables (Pourghasemi et al., 2013). This method addresses the limitations of traditional linear regression, which is constrained to continuous variables. In contrast, in the GWR model, local regression equations are established at each point within a spatial extent, exploring spatial variations at a specific scale. This method allows for dynamic updates of habitat factor weights across different regions. However, GWR is limited to continuous variables. We leveraged the strengths of both the GWR and LR models, considering landscape and spatial heterogeneity to establish a large-scale grasshopper habitat suitability monitoring model in China (CL-GWLR). The calculation method is outlined as follows:

$$P(Y=1) = \frac{\exp(\alpha_{0(u_i,v_i)} + \alpha_{1(u_i,v_i)}x_{i1} + \alpha_{2(u_i,v_i)}x_{i2} + \ldots + \alpha_{n(u_i,v_i)}x_{in})}{1 + \exp(\alpha_{0(u_i,v_i)} + \alpha_{1(u_i,v_i)}x_{i1} + \alpha_{2(u_i,v_i)}x_{i2} + \ldots + \alpha_{n(u_i,v_i)}x_{in})} = \frac{1}{1 + \alpha_{0(u_i,v_i)} + \alpha_{1(u_i,v_i)}x_{i1} + \alpha_{2(u_i,v_i)}x_{i2} + \ldots + \alpha_{n(u_i,v_i)}x_{in}} \tag{2-2}$$

The probability of grasshopper occurrence at the location is denoted as P, and the probability of no grasshopper occurrence at the same location is denoted as $(1 - P)$.

After applying the Logit transformation, we have

$$\text{Logit(P)} = \ln\frac{P}{1-P} = \alpha_{0(u_i,v_i)} + \alpha_{1(u_i,v_i)}x_{i1} + \alpha_{2(u_i,v_i)}x_{i2} + \ldots + \alpha_{n(u_i,v_i)}x_{in} \tag{2-3}$$

Finally, the parameters of the local regression model for the location are obtained using the weighted least-squares method.

$$_{(u_i,v_i)} = \left(X^T W(u_i,v_i)X\right)^{-1} X^T W(u_i,v_i)\text{logit}(P), \tag{2-4}$$

where (u_i, v_i) are the geographical coordinates of i,$\alpha_{0(u_i,v_i)} + \alpha_{1(u_i,v_i)}x_{i1} + \alpha_{2(u_i,v_i)}x_{i2} + \ldots + \alpha_{n(u_i,v_i)}x_{in}$ is the estimated value; $W(u_i, v_i)$ is the matrix weight; and X represents the matrix of explanatory variables.

To compare the accuracy of these models, we used the CL-GWLR, GWLR, and OLS models to determine the optimal method for monitoring grasshopper habitats. The model performance was evaluated using the Akaike Information Criterion (AIC) and R^2. Lower AIC values signified better model fitting, whereas higher R^2 values indicated a better explanation of the independent variables based on the dependent variables, reflecting stronger model interpretability.

The monitoring results of grasshoppers were classified into three levels based on the probability of occurrence: less suitable ($0 < P \leq 0.5$), moderately suitable ($0.5 < P \leq 0.7$), and most suitable ($0.7 < P \leq 1$) (Guo et al., 2023). The spatiotemporal evolution of suitable grasshopper habitats was then analyzed to reveal the driving factors behind their spatiotemporal changes.

3. Results

3.1. Construction of a grasshopper habitat monitoring indicator system

Based on the grasshopper developmental and growth mechanism, combined with spatio-temporal continuous multisource data, the grasshopper habitat monitoring indicator system (Fig. 3) was constructed by using difference tests, correlation analysis, and importance tests. Based on the developmental mechanisms of grasshoppers, we used the DD model to estimate the developmental periods of dominant grasshopper species across various regions. The findings (Fig. 3A) revealed notable similarities in the developmental progress of the same grasshopper species across different regions, whereas significant differences were observed among species. The monitoring results for the nymph stage indicated that *O. chinensis* in the HLJ region had the longest duration, spanning 73 days, followed by *C. italicus* in the XJ region, with a duration of 69 days. To understand the extended nymph stages of *O. chinensis* and *C. italicus*, hourly temperature data were analyzed. The results showed that regions with significant diurnal temperature variations accumulated effective thermal energy primarily during the daytime, necessitating a longer period to meet the energy requirements for nymph development. For *Oedaleus*, minimal differences in developmental progress were observed between *O. decorus asiaticus* in the GSNI and HJLK regions. However, in the SX region, *O. infernalis* exhibited nymph and adult stages that were approximately 15 and 10 days longer than those of *O. decorus asiaticus* in the GSNI and HJLK regions, suggesting notable interspecific developmental differences. Among all species, *C. dubius* in the QH region had the shortest nymph period, lasting 32 days. This is likely because *C. dubius* has only four instars, compared to the five or six instars observed in other grasshopper species.

The results of the variance analysis on the monitoring indicators (Fig. 3B) indicated that the minimum temperatures during the egg stage (EMinT) in the non-occurrence areas of *O. decorus asiaticus* and *O. infernalis* were higher than those in the occurrence areas. Specifically, the EMinT for *O. decorus asiaticus* ranged from −32 °C to −20 °C, while those for *O. infernalis* ranged from −22 °C to −16 °C. These findings suggest that excessively high overwintering temperatures are not conducive to the growth and development of *Oedaleus* species, which thrive under relatively low-temperature conditions. Additionally, the EMinT of *O. infernalis* was higher than that of *O. decorus asiaticus*, indicating a relatively stronger cold tolerance of *O. decorus asiaticus*. Analysis of habitat factors for *D. barbipes* in the HL and XW regions revealed a preference for areas with slopes ranging from 1° to 2° because

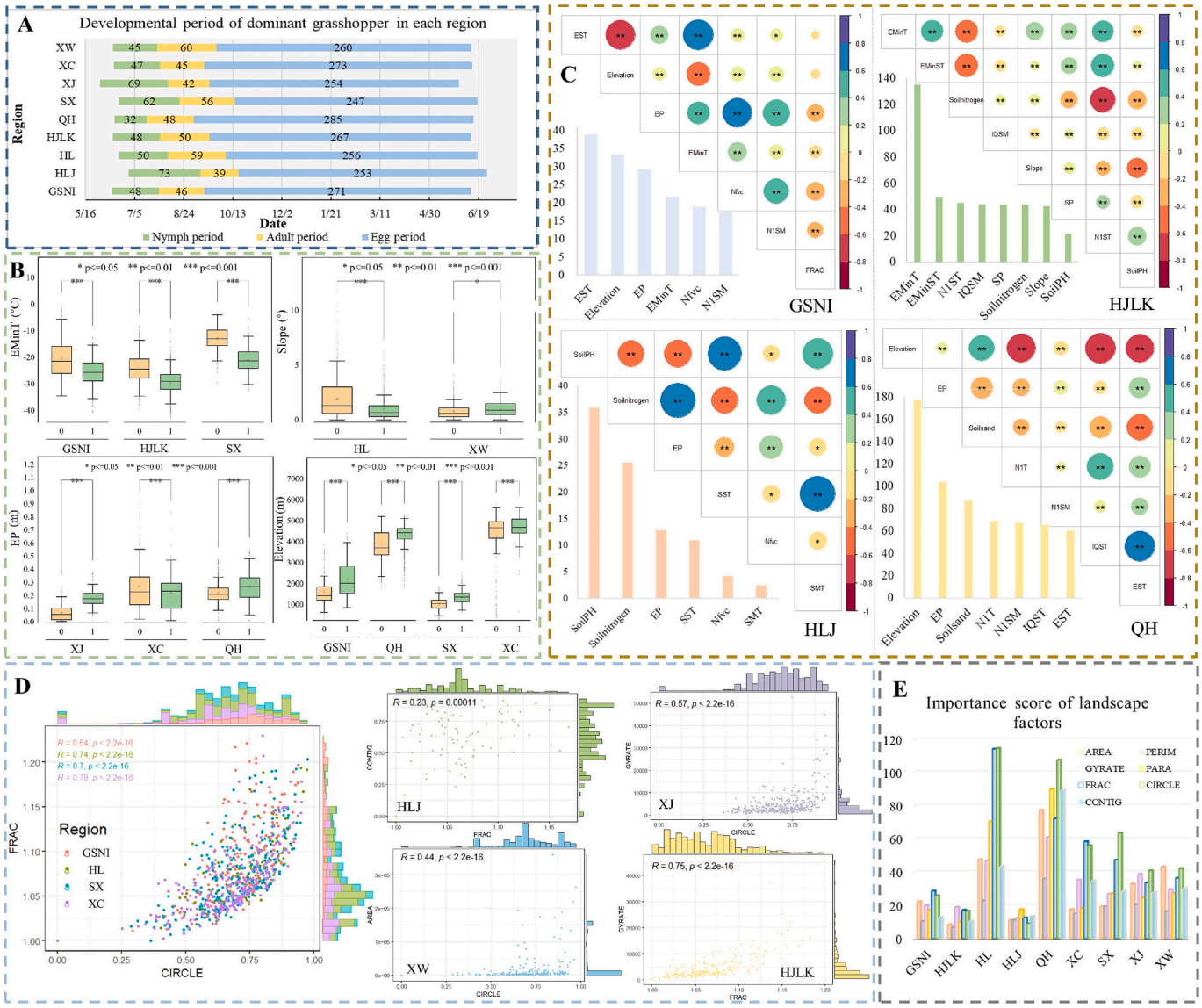

Fig. 3. Results of the seven dominant grasshopper habitat monitoring indicator systems for China; (a) Calculation results of the developmental stages of seven dominant grasshoppers in nine niche subregions; (b) Test results of factors with significant differences; '0' indicates the non-occurrence of grasshoppers and '1' represents their occurrence. (c) Analysis of local habitat factor correlations and importance test results. The correlation relationship among main variables is shown upper and the importance test results are lower with the bar chart; (d) Results of landscape variables correlation analysis. The scatter plots represent the distribution of each variable and the correlation relationship is presented as R and p-value; (e) Importance test results of landscape factors. The x-axis represents the name of each region, while the y-axis stands for the importance test score.

steeper slopes were less suitable for grass growth thereby it is not suitable for grasshopper survival. Precipitation during the egg period (EP) was higher in grasshopper occurrence areas of the XJ and QH regions (0.15–0.25 m and 0.2–0.32 m, respectively) compared to non-occurrence areas. In the XC region, the EP in the occurrence areas of *L. migratoria tibetensis* was slightly lower than in the non-occurrence areas but was still primarily concentrated between 0.15 and 0.3 m. Elevation analysis revealed that the mean elevation of grasshopper occurrence areas in the GSNI, QH, SX, and XC regions is higher than that of non-occurrence areas. Specifically, the occurrence areas of *C. dubius* and *L. migratoria tibetensis* in QH and XC occurred at elevations between 4,000 and 5,000 m, whereas *O. decorus asiaticus* and *O. infernalis* were mainly found at 1000–3000 m and 1000–2000 m, respectively. The higher elevations of *C. dubius* and *L. migratoria tibetensis* habitats reflect their adaptation to the extreme conditions of the Tibetan Plateau.

Correlation and importance analyses (Fig. 3C) revealed that, for the same grasshopper species, the weights of the influencing factors varied across regions. For *O. decorus asiaticus*, the surface and soil temperatures during the egg stage were the critical factors. However, in the GSNI region, the mean soil temperature during the egg stage (EST) and minimum surface temperatures during the egg stage (EMinT) contributed more significantly, whereas, in the HJLK region, EMinT and minimum soil temperature in the egg stage (EMinST) played more crucial roles. Elevation played a decisive role in the distribution of *O. decorus asiaticus* in the GSNI region, whereas slope had a greater contribution to the distribution of *O. decorus asiaticus* in the HJLK region. For *O. chinensis* in the HLJ region, soil pH and nitrogen content were key factors due to the prevalence of nutrient-rich black soil in the region (Xia et al., 2010). Elevation also plays a significant role in the occurrence of *C. dubius* on the Tibetan Plateau, with an average elevation of 4,058.40 m, which is notably higher than that of other regions. Under such extreme environmental conditions, elevation is the most critical factor influencing the occurrence of grasshoppers.

Correlation (Fig. 3D) and importance analyses (Fig. 3E) of landscape

factors revealed that FRAC and CIRCLE exhibited high importance but low correlation (R < 0.8) in the GSNI, HL, SX, and XC regions. These two metrics, which represent the patch shapes of vegetation types, are effective in assessing the characteristics of patch shapes in these regions. In the HLJ region, CONTIG and FRAC were incorporated into the monitoring indicator system. The CONTIG represents landscape aggregation, whereas the FRAC reflects patch-shape complexity. Together, these indicators effectively capture the landscape habitat characteristics of the HLJ region. In XJ, the landscape edge indicator GYRATE and the shape indicator CIRCLE also showed low correlation and high importance. Combining these two metrics provides an accurate representation of the patch features of the vegetation types in XJ. In the XW region, the AREA and CIRCLE reflect the area and shape of the landscape, respectively. These indicators are crucial to understanding the occurrence and distribution of grasshoppers in a region. In the HJLK region, landscape shape indicators GYRATE and FRAC were used for subsequent analyses. FRAC is included in the final indicator system for regions with higher grassland fragmentation. This metric effectively represents landscape complexity and reflects the habitat characteristics of these areas. The final monitoring indicators for each region are shown in Fig. S1.

3.2. Spatiotemporal patterns of the distribution of dominant grasshoppers

3.2.1. Spatial and temporal patterns of grasshopper occurrence across China

Moran's I was used to assess the global spatial autocorrelation of grasshopper occurrence. The results (Fig. S2) show that, within a 99 % confidence interval, the z-scores of grasshopper occurrences across years range from 13.21 to 70.74, all exceeding 1.65 with p-values <0.01. These findings confirm that grasshopper occurrence is non-random and exhibits significant spatial autocorrelation. Building on this global analysis, we further explored the local spatial characteristics and HAGs. The results (Fig. 4) demonstrated a clear aggregation pattern of HAGs from 2019 to 2023, with a progressive shift from southwestern to northeastern China. The primary HAGs were located in the northwest HJLK and XJ, western HL, eastern QH, northeastern XW, and southwestern XC. These regions offer the most favorable environments for grasshopper breeding and reproduction, requiring close monitoring for the occurrence of grasshoppers in these areas. A year-by-year analysis of HAGs revealed notable spatial dynamics. In 2019, the primary HAGs were concentrated in the northwest HJLK and east XW, reflecting significant aggregation patterns of *O. decorus asiaticus* and *D. barbipes*. By 2020, the spatial extent of HAGs expanded further along the east–west direction, driven by a more pronounced clustering of hotspots in XJ compared to previous years. In 2021, the contraction of HAGs in Sichuan Province resulted in a north–south aggregation pattern, with key areas located in the border regions of HJLK and XW, western HL, and northeastern QH. By 2022, the HAGs in XC and XJ exhibited further contractions, with the main hotspots shifting to HL, HJLK, and XW. In 2023, the clustering of grasshopper occurrences became more pronounced in HJLK, QH, XC, and XJ, resulting in the southwestward expansion of HAGs. An analysis of the HAGs distributions and migration of occurrence centers across regions (Fig. 5) revealed that the central locations of grasshopper occurrences predominantly occupied the GSNI and XW regions. From 2019 to 2021, the center of occurrence was located in the northeastern part of GSNI. In 2022, the center shifted northeastward to the GSNI-XW border. By 2023, it migrated southwest and returned to the GSNI region.

3.2.2. Spatial and temporal patterns of o. Decorus asiaticus and D. Barbipes occurrence

The monitoring results for the two aggregation areas of *O. decorus asiaticus* revealed significant trends in spatial distribution over multiple years. In the HJLK region, the center of occurrence in 2019 was located in the northwest, with a general aggregation pattern extending from the southwest to the northeast. By 2020, the occurrence center had shifted southward, accompanied by a north–south expansion of the HAG. In the GSNI region, hotspots for *O. decorus asiaticus* were primarily concentrated in the southern part of the Gansu Province (Fig. 4). Notably, the occurrence center exhibited a consistent eastward migration trend in most years (except between 2020 and 2021), this suggests a sustained eastward expansion of *O. decorus asiaticus* within the GSNI region. These findings underscore the importance of monitoring its occurrence in both northwestern HJLK and eastern GSNI.

In the HL region, the primary HAGs were located on the four western banners of Hulunbuir City, with the most extensive distribution observed in 2019. By 2020, the hotspot areas had contracted and shifted westward, indicating a more concentrated distribution of *D. barbipes*

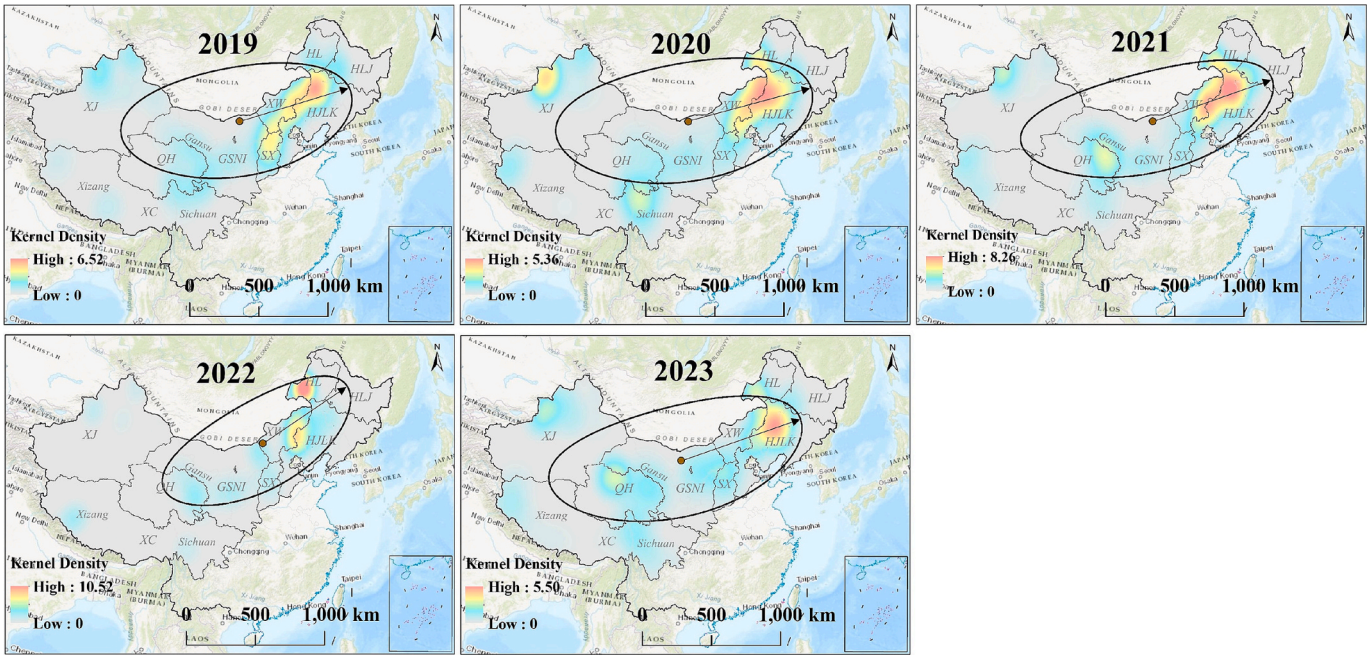

Fig. 4. Spatial pattern of grasshopper occurrence in China from 2019 to 2023. The ellipse represents the standard deviation ellipse of grasshopper occurrence.

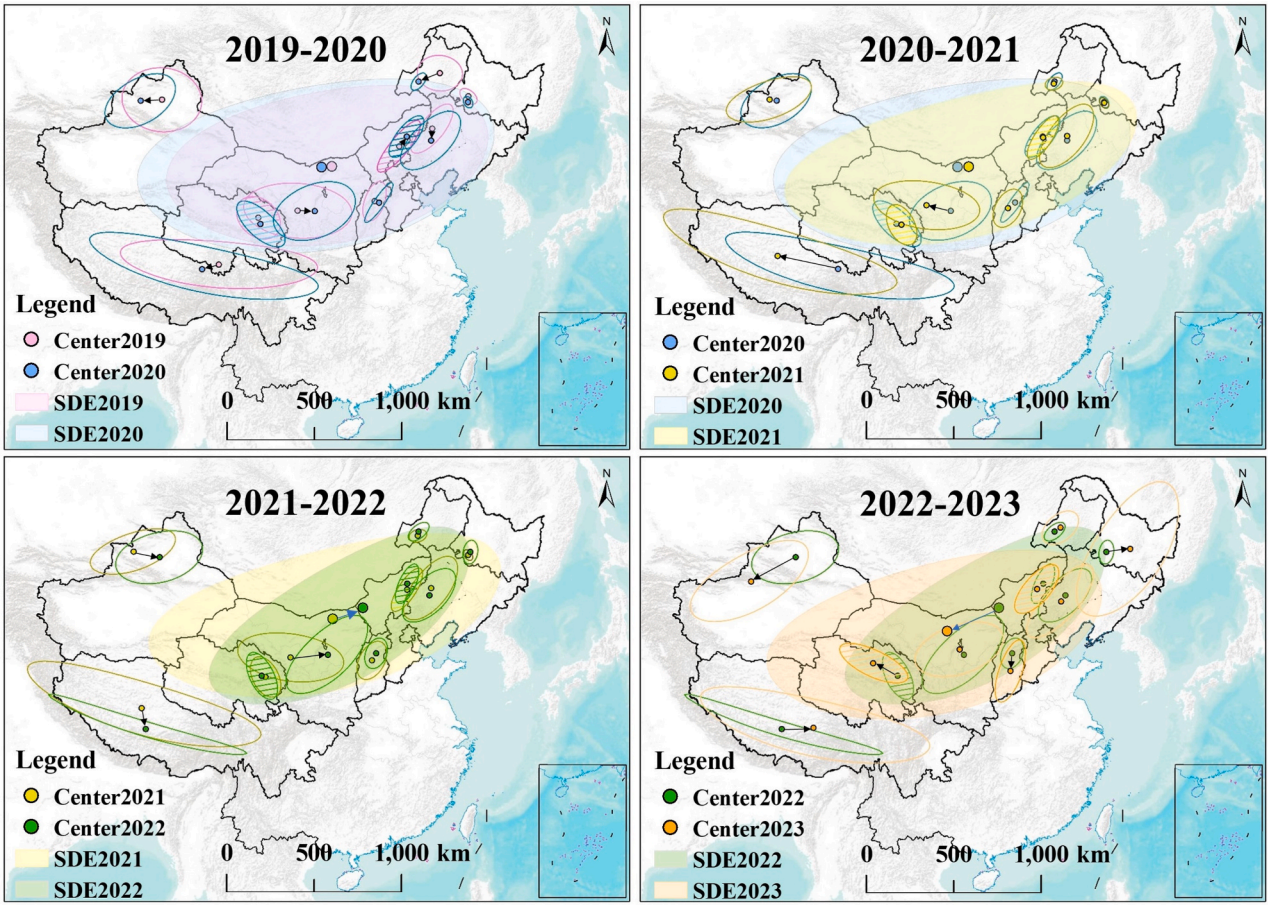

Fig. 5. Temporal pattern of grasshopper occurrence in China from 2019 to 2023. Large and small points represent the mean center of grasshopper occurrence in China and each region, respectively. Blue and black arrows indicate the direction of mean center changes in China and each region, respectively. To more explicitly show the changes in each region, Xingol League and Ulanqab City (XW), Qinghai (QH), and Heilongjiang (HLJ) are labeled with a slash. (For interpretation of the references to colour in this figure legend, the reader is referred to the web version of this article.)

within the HL region. In 2022, *D. barbipes* showed the most pronounced aggregation, highlighting the need to monitor population density to prevent the formation of high-density spots. From 2022 to 2023, hotspot areas gradually expanded northeastward, necessitating further investigation into the occurrence of *D. barbipes* in northeastern HL. In the XW region, hotspot areas of *D. barbipes* were primarily located in eastern XW, including Xilinhot City and the West and East Ujimqin Banners, and remained relatively stable between 2020 and 2022. However, from 2022 to 2023, the HAGs expanded southwest. Analysis of HAGs in both XW and HL regions revealed an expansion trend in 2023 (Fig. 5), emphasizing the need for vigilant monitoring of outbreaks in northeastern HL and southwestern XW.

3.2.3. Spatial and temporal patterns of the occurrence of other dominant grasshoppers

The hotspots for *C. dubius* were primarily located in the northeastern QH, along the border with Gansu. Spatial analysis revealed that in 2021, this species exhibited the most pronounced aggregation, despite having the smallest aggregation area. By 2023, the aggregation area expanded, with the center of occurrence shifting northwestward, emphasizing the need for close monitoring of *C. dubius* in the northwestern QH region. In the XC region, *L. migratoria tibetensis* is predominantly distributed in southwestern Tibet and northwestern Sichuan Province. From 2019 to 2021, HAGs expanded from east to west, whereas between 2021 and 2022, the hotspot areas contracted, with a more distinct north-to-south aggregation. From 2022 to 2023, increased aggregation in northern Sichuan prompted further northeastward expansion of HAGs in XC. This emphasizes the need for increased attention to the occurrence of *L. migratoria tibetensis* in northern Sichuan. For *C. italicus* in the XJ region, hotspots were situated in the northern administrative divisions of Xinjiang near the border of Kazakhstan. From 2019 to 2020, the aggregation area became more concentrated, with the occurrence center shifting eastward. Between 2021 and 2022, the center shifted southeastward, and from 2022 to 2023, it moved southwestward, accompanied by further HAG expansion. This trend reflected the more dispersed distribution of *C. italicus* in southwestern XJ. *O. infernalis* is primarily concentrated in central and northern SX. The extent of the aggregated areas remained relatively stable across most years, except between 2022 and 2023, when the occurrence center shifted southward, accompanied by the southward expansion of HAGs. This shift underscores the need for increased attention to the occurrence of *O. infernalis* in southern SX. *O. chinensis* was mainly concentrated in southwestern HLJ, with the largest HAGs observed in 2023. This indicated a shift in the aggregation trend of *O. chinensis* in the HLJ region, with a marked northeastward movement.

3.3. Monitoring results for grasshopper habitats

The CL-GWLR model considers both spatial heterogeneity and landscape characteristics and dynamically adjusts the weights of habitat factors in complex environments. Its performance was evaluated against the OLS model, which neglects spatial heterogeneity, and the GWLR model, which omits landscape factors. Model accuracy was assessed using AIC and R^2. The results (Table 1) showed that the model

Table 1
Monitoring accuracy of suitable grasshopper habitats from 2019 to 2023.

2019										
		GSNI	**HJLK**	**HL**	**HLJ**	**QH**	**SX**	**XC**	**XJ**	**XW**
OLS	AIC	87.77	163.19	196.45	20.91	162.15	71.08	147.25	48.25	126.24
	R^2	0.37	0.22	0.32	0.88	0.20	0.59	0.228	0.81	0.33
GWLR	AIC	85.45	148.47	134.96	17.75	83.96	67.71	107.40	44.77	113.97
	R^2	0.43	0.36	0.68	0.88	0.71	0.62	0.65	0.83	0.47
CL- GWLR	AIC	81.57	139.21	127.52	17.08	89.20	54.68	102.37	42.13	107.03
	R^2	0.50	0.40	0.72	0.88	0.72	0.72	0.68	0.84	0.48
2020										
		GSNI	**HJLK**	**HL**	**HLJ**	**QH**	**SX**	**XC**	**XJ**	**XW**
OLS	AIC	70.74	60.04	340.20	21.99	464.21	43.70	114.31	97.04	63.93
	R^2	0.41	0.69	0.23	0.85	0.23	0.68	0.22	0.51	0.73
GWLR	AIC	66.26	62.87	196.84	18.08	223.64	40.26	94.31	99.52	60.56
	R^2	0.49	0.72	0.67	0.87	0.69	0.75	0.55	0.52	0.73
CL- GWLR	AIC	64.78	60.97	195.22	17.25	208.32	37.85	68.05	95.98	46.85
	R^2	0.52	0.73	0.68	0.89	0.73	0.78	0.75	0.57	0.77
2021										
		GSNI	**HJLK**	**HL**	**HLJ**	**QH**	**SX**	**XC**	**XJ**	**XW**
OLS	AIC	86.91	241.10	216.53	17.91	295.53	120.82	136.44	81.73	98.52
	R^2	0.41	0.32	0.32	0.89	0.35	0.46	0.27	0.65	0.35
GWLR	AIC	63.83	218.86	120.43	18.13	156.27	111.37	116.44	83.67	96.02
	R^2	0.72	0.50	0.74	0.86	0.72	0.64	0.59	0.70	0.41
CL- GWLR	AIC	59.75	212.12	119.46	17.04	156.04	112.85	114.80	66.40	86.11
	R^2	0.81	0.64	0.77	0.91	0.74	0.75	0.61	0.77	0.49
2022										
		GSNI	**HJLK**	**HL**	**HLJ**	**QH**	**SX**	**XC**	**XJ**	**XW**
OLS	AIC	99.86	145.25	316.16	40.11	348.15	49.24	146.51	80.05	139.78
	R^2	0.23	0.36	0.16	0.80	0.20	0.73	0.39	0.65	0.44
GWLR	AIC	97.52	124.72	96.54	42.95	147.61	45.28	101.03	79.37	157.89
	R^2	0.35	0.60	0.83	0.81	0.76	0.77	0.68	0.50	0.45
CL- GWLR	AIC	92.56	122.12	95.94	37.32	157.80	42.05	99.59	54.78	143.32
	R^2	0.40	0.63	0.84	0.83	0.78	0.80	0.72	0.71	0.52
2023										
		GSNI	**HJLK**	**HL**	**HLJ**	**QH**	**SX**	**XC**	**XJ**	**XW**
OLS	AIC	58.20	157.67	132.48	17.76	299.45	37.82	164.13	71.28	209.64
	R^2	0.38	0.32	0.44	0.90	0.25	0.84	0.17	0.56	0.19
GWLR	AIC	66.70	133.97	74.28	36.41	222.87	47.23	77.24	59.60	233.14
	R^2	0.31	0.63	0.80	0.80	0.55	0.83	0.73	0.62	0.22
CL- GWLR	AIC	53.61	131.88	62.15	17.53	168.30	44.52	81.69	50.90	203.87
	R^2	0.67	0.64	0.86	0.90	0.67	0.86	0.74	0.68	0.24

accounting for spatial heterogeneity significantly outperformed the traditional OLS model, highlighting the limitations of ignoring spatial heterogeneity in monitoring grasshopper habitats. Among the two spatially heterogeneous models, the CL-GWLR model consistently achieved lower AIC values and higher R^2 values for GSNI, HJLK, HL, HLJ, SX, XJ, and XW over the past five years, indicating superior performance compared to the GWLR model. In specific cases, such as the QH region in 2019 and 2022 and the XC region in 2023, the AIC values of the CL-GWLR model were slightly higher than those of the GWLR model. However, the CL-GWLR model consistently achieved higher R^2 values, indicating a better overall fit. Based on a comprehensive evaluation of accuracy across all regions over the past five years, the CL-GWLR model outperformed both the OLS and GWLR models. Consequently, the CL-GWLR model was used to monitor suitable grasshopper habitats.

Monitoring results of the CL-GWLR model, along with the area and proportion of habitats at each suitability level for each year, are shown in Fig. 6. The analysis reveals that the most suitable habitats for grasshoppers ranged from 1,467.25 million mu to 1,809.49 million mu, accounting for 31–38 % of the total grassland area. These habitats were primarily concentrated in northwestern HJLK, northern and eastern XW bordering HJLK, western HL, northern and western XJ, southwestern GSNI and XC, and northeastern QH. In particular, the most suitable habitats for *C. italicus* in XJ and *L. migratoria tibetensis* in XC were both located near the border areas. Close attention should be paid to grasshopper outbreaks in these regions, highlighting the need for vigilant monitoring to mitigate the risk of cross-border migration. Moderately suitable areas vary from 450.81 to 747.52 million mu, accounting for 11–16 % of the total grassland area. These areas are primarily distributed in northwestern XC, central QH, and eastern GSNI. In 2022, the most suitable habitat area was the smallest, whereas the moderately suitable area was the largest. This shift can be probability attributed to the transition of the most suitable areas in northwestern XC into moderately suitable areas, and the conversion of less suitable areas in the eastern GSNI into moderately suitable areas. In 2023, the most suitable habitat area was the largest, and the less suitable habitat was the smallest. Statistical analysis of habitat areas across regions (Fig. 7) demonstrated that the increase in the most suitable areas was driven primarily by expansion in the GSNI, HJLK, and HL regions. The most suitable habitats in these areas accounted for more than 50 % of the total regional grassland area. These regions were predominantly inhabited by *O. decorus asiaticus* and *D. barbipes*, which are frequently involved in grasshopper outbreaks. Therefore, it is essential to closely monitor grasshopper population dynamics in these regions to prevent large-scale outbreaks.

The Fig. 6 shows that QH and XC had the largest grassland areas. Because of their lower temperatures and limited precipitation, these regions provide favorable conditions for the growth of herbaceous plants, resulting in vast expanses of grasslands. However, the proportion of the most suitable habitat area for grasshoppers is relatively low, with 50–60 % of the environment being unsuitable for grasshopper breeding. Effective management practices have further suppressed grasshopper population density, making them less prone to severe grasshopper outbreaks. Conversely, the most severe grasshopper outbreaks have been reported in the HJLK, HL, XJ, and XW regions, according to data from the National Forestry and Grassland Administration. The lower altitudes and proximity of these regions to international borders facilitate large-scale annual grasshopper migration from neighboring countries. Combined with favorable habitat conditions, these factors contribute to a

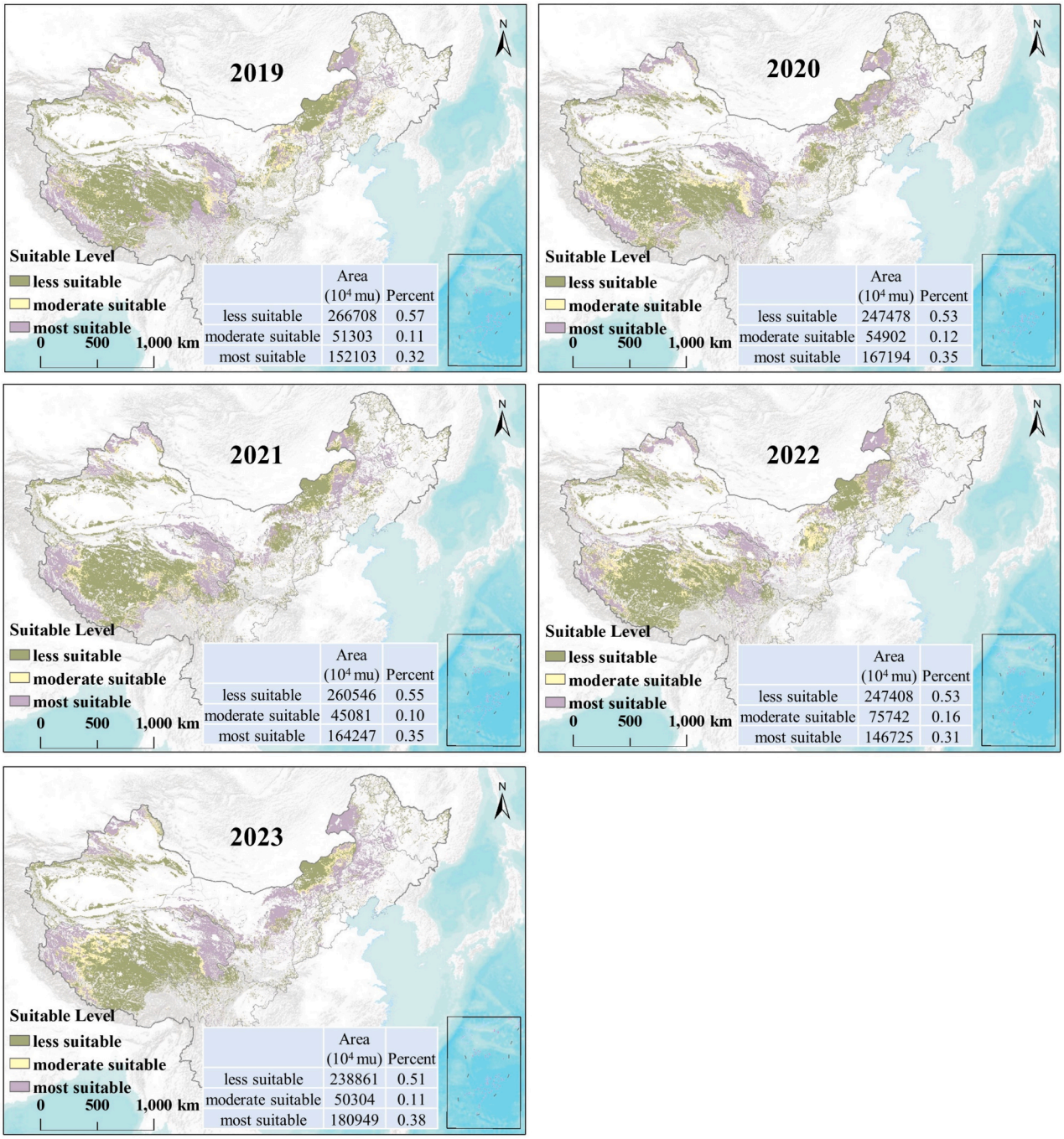

Fig. 6. Monitoring results of grasshopper habitat in China considering spatial heterogeneity and landscape factors.

higher severity of outbreak.

The monitoring results further revealed that the most suitable habitats for grasshoppers in HJLK were primarily concentrated in the northwestern region, particularly in the Kerqin grassland area. This region, dominated by *Stipa grandis* and *Leymus chinensis*, provides optimal conditions for the habitat and reproduction of *O. decorus asiaticus*. From 2019 to 2021, the most suitable habitats remained relatively stable and were primarily located in the northeastern region. However, in 2022, the proportion of most suitable habitats dropped to 36 % due to habitat transitions in the central region. In 2023, recovery in central HJLK increased the proportion of most suitable habitats by 32 %, reaching the highest proportion on record. The most suitable habitats in HL were predominantly in the western region. From 2019 to 2021, the proportion of most suitable habitats gradually decreased from 58 % to 41 %. However, subsequent recovery from 2021 to 2023 indicated improved conditions for *D. barbipes*. This trend underscores the need for close monitoring of *D. barbipes* outbreaks in this region. XW and HL are geographically close, and both regions provide favorable conditions for the survival and reproduction of *D. barbipes*. Monitoring of suitable areas in XW revealed that the most suitable habitats were in the eastern regions. The grassland distribution map (Fig. 1) shows that western XW is dominated by desert grassland, which has low vegetation cover and fails to meet the normal feeding requirements of *D. barbipes*. Therefore, this area is unsuitable for the growth and development of grasshoppers. In contrast, central and eastern XW are dominated by typical and meadow steppes, with vegetation coverage ranging from 20 % to 50 %. These areas provide sufficient sunlight and adequate food sources, making them suitable for grasshopper growth and reproduction. In 2019, the

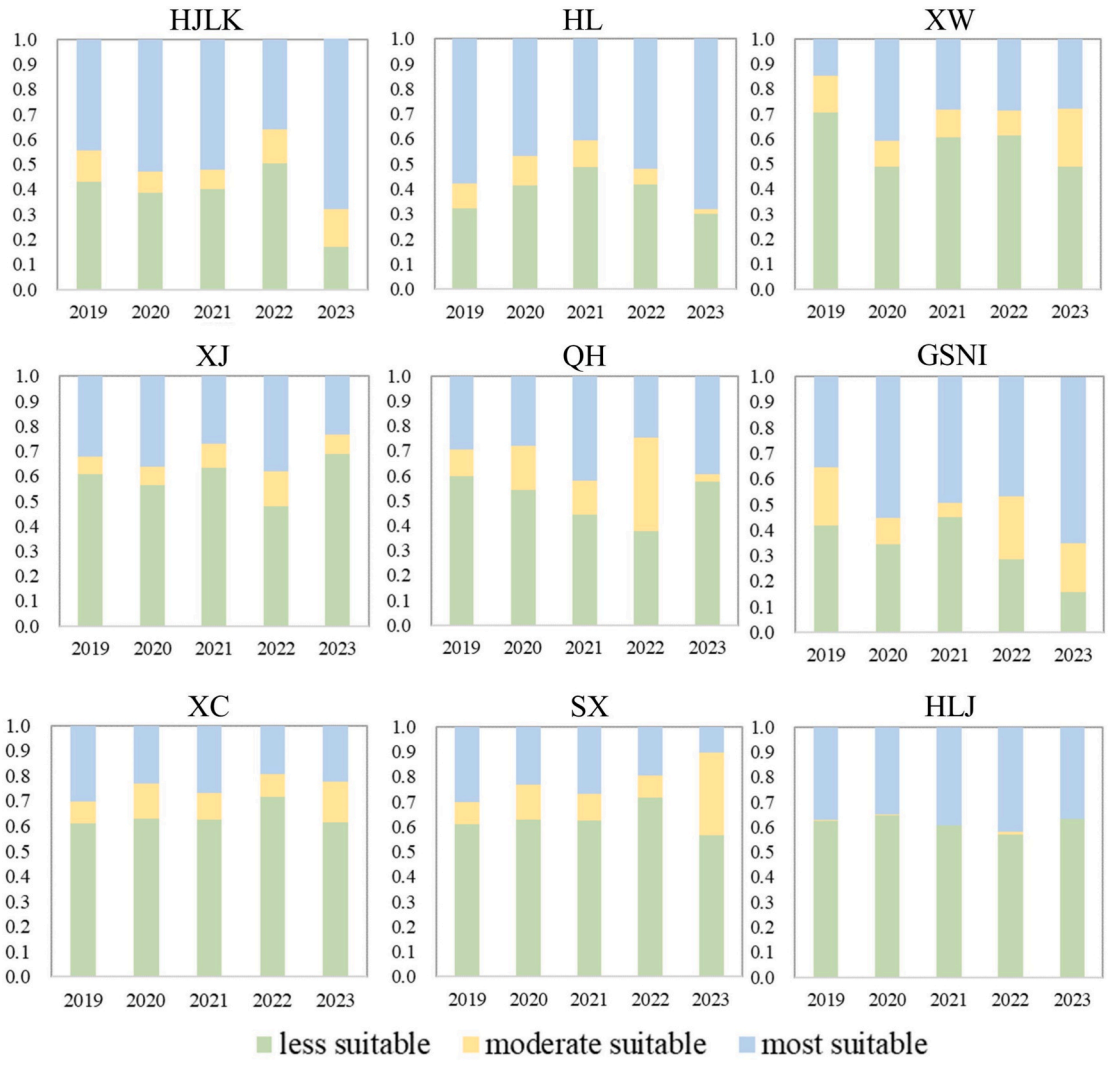

Fig. 7. Proportion of habitat suitability levels for grasshoppers in each region.

most suitable habitat area for XW was 15 %. However, by 2020, the proportion increased by 26 %, primarily because of the transition of moderately suitable areas in the northern and eastern regions into the most suitable habitats. From 2021 to 2023, the proportion of most suitable habitats remained stable at 28 %. In XJ, *C. italicus* was concentrated in border areas, with habitat suitability fluctuating between 23 % and 28 %. While central and western XJ exhibited stable suitability, northern Altai experienced a decline in habitat suitability between 2022 and 2023, shifting from the most suitable to less suitable areas. The proportion of most suitable habitats in the GSNI ranged from 36 % to 68 %. The smallest proportion occurred in 2019; however, by 2020, the northeastern GSNI transitioned to become a more suitable habitat, leading to a 19 % increase in their proportion. In 2023, eastern GSNI reached the largest suitable habitat areas. This highlights the importance of monitoring *O. decorus asiaticus* in this region. In the HLJ region, the most suitable habitat for *O. chinensis* remained relatively stable and was primarily concentrated in the southeastern region. In SX, *O. infernalis* habitats were primarily located in the central and northern areas, with suitable habitats ranging from 12 % to 29 %. Monitoring remains crucial for preventing population surges in these regions.

4. Discussion

4.1. Effectivity of the dynamic model for grasshopper habitat monitoring

In this study, based on the multi-source remote sensing and ecology data, we established a monitoring indicator system for seven dominant grasshopper species based on their growth and developmental mechanisms. Additionally, we explored the spatiotemporal distribution patterns of grasshopper occurrence and developed a dynamic large-scale monitoring model for suitable habitats, accounting for landscape characteristics and spatial heterogeneity. The methodological contributions of this study are as follows: First, it systematically integrated the developmental mechanisms of dominant grasshopper species using a DD model to examine their developmental cycles across different regions. Compared to the research that relies solely on empirical estimations (Du et al., 2022; Zhang et al., 2023), our approach provides a more precise framework for selecting the temporal ranges of environmental factors than traditional methods. Second, the interactions between grasshopper occurrence, host plants, and environmental conditions were quantitatively analyzed. Compared to localized empirical methods (Tappan et al., 1991; Sun et al., 2023), our approach demonstrated more systematic. Moreover, the differences in dominant indicators were evident across species: temperature during the egg stage exhibited more importance for *Oedaleus* species compared to others, with *O. decorus asiaticus* demonstrating greater cold tolerance than *O. infernalis*. These

findings are similar to Colvin (1997), who identified temperature during the egg stage as a critical determinant for *Oedaleus* survival and development. Elevation plays a vital role in *C. dubius* distribution, consistent with documented critical elevational constraints in its habitat selection (Loughman, 2010; Allison et al., 2022). Additionally, we delineated the spatiotemporal patterns of HAG distribution across China. Our results showed significant spatial autocorrelation within a 99 % confidence interval of HAGs, providing a scientific basis for the sustainable management of grasshoppers in grassland ecosystems. The results are similar to Badenhausser's (2012) findings, which found spatial autocorrelation at the 95 % confidence interval in grasshoppers in western France. Furthermore, we integrated the landscape characteristics of 223 vegetation types and incorporated spatial heterogeneity to construct a dynamic large-scale habitat monitoring model with adaptive weight updating for habitat factors. Compared with traditional models that do not consider landscape features or spatial heterogeneity (Guo et al., 2023; Geng et al., 2020), the proposed model significantly improves monitoring accuracy and better delineates the potential distribution of grasshoppers. These results provide valuable information for field investigations of grasshopper habitats.

4.2. Driving factors for hotspot areas and suitable habitat changes

From 2019 to 2020, the HAG in northeastern XW became more concentrated as the region transitioned from a less suitable to a most suitable habitat. Analysis of the driving factors behind these changes indicated that changes in this region were primarily influenced by meteorological conditions. The synergistic effects of EP and N4T play a key role in shaping suitable habitats. In 2019, N4T reached 42.25 °C (Fig. 8A), while EP was only 0.027 m. Insufficient precipitation during the egg period caused desiccation of grasshopper eggs, while the exceptionally high temperatures during the fourth- and fifth-instar nymph stages disrupted normal physiological activities. The combined effects of these two factors led to the contraction of suitable habitat areas. Between 2021 and 2022, the HAG in northwestern HJLK experienced a reduction. Suitable habitat areas transitioned from the most suitable to less suitable for *O. decorus asiaticus*, resulting in fewer favorable environments and contraction of the HAG range. Further analysis indicated that the EMinT in northeastern HJLK in 2022 was only –23.93 °C, while the SP reached 0.11 m (Fig. 8B). The combination of relatively high temperatures during the oviposition period and excessive precipitation during the egg stage likely caused water oversaturation in eggs, which adversely affected their survival. This environmental shift contributed to the contraction of the HAG and a decline in habitat suitability. In 2023, the distribution of HAGs reached its widest extent, with the highest recorded proportion of the most suitable areas. In particular, conditions suitable for grasshopper habitation and reproduction in 2023 underscore the need for close monitoring of population dynamics. In the eastern GSNI, habitat suitability transitioned from less suitable to moderately suitable, and finally to most suitable. The combination of favorable EP (0.05–0.07 m), EST (2.09–2.4 °C), and fractional vegetation cover during the nymph period (Nfvc: 0.2–0.3) created increasingly suitable environmental conditions for grasshopper habitation and reproduction. Consequently, HAG reached its maximum extent and showed significant improvements in habitat suitability.

4.3. Uncertainties and improvements of multi-source remote sensing data in grasshopper habitat monitoring

This paper integrates multi-source remote sensing data to establish a comprehensive monitoring indicator system, utilizing MODIS, ERA5_-Land, SoilGrids, and DEM data. Based on these indicators, a habitat monitoring model for grasshoppers was developed, achieving high accuracy. However, several uncertainties still require further clarification. First, the habitat parameters derived from multi-source data can introduce uncertainties (Zhang et al., 2020). The dynamics of the grasshopper life cycle are influenced by a variety of meteorological, vegetative, soil, and topographic factors obtained from different sensors. Methodological inconsistencies in data acquisition, especially differences between optical sensors (e.g., MODIS) and microwave sensors (e.g., SMAP for soil moisture) can create systematic biases in the derived parameters, ultimately affecting the model's accuracy. Second, inconsistencies in temporal resolution also present challenges (Nagendra et al., 2013). Even among sensors operating within the same platform, such as MODIS, there are disparities in temporal resolutions. The MOD11A1 dataset provides daily land surface temperature data, while MOD13A2 offers 16-day composites of vegetation indices. This difference in compositing duration may obscure critical rapid vegetation green-up phases that coincide with nymphal emergence, thereby affecting the model accuracy. Finally, there are limitations associated with coarse spatial resolution (McPherson et al., 2006; Lecours et al., 2015). Large-scale environmental data often fail to capture the spatial heterogeneity of grasshopper microhabitats. In this study, the 1 km resolution of remote sensing data may inadequately represent grasshopper activity ranges <1 km^2, particularly for microhabitat features such as <10 m^2 vegetation patches that are suitable for oviposition.

Future research can be further improved in the following three aspects: (1) This study only focused on seven dominant grasshopper species; there are over 400 species of grasshoppers across China's grasslands. Future studies should incorporate additional dominant species for a more comprehensive analysis. (2) While the current study employs a 1 km spatial resolution, future research should prioritize the adoption of finer resolutions (e.g., 30 m) to better resolve microhabitat heterogeneity. (3) The study period spanned from 2019 to 2023. In future research, incorporating long-term historical data on grasshopper occurrence would allow for a more representative monitoring system and facilitate the analysis of spatiotemporal patterns in habitat suitability.

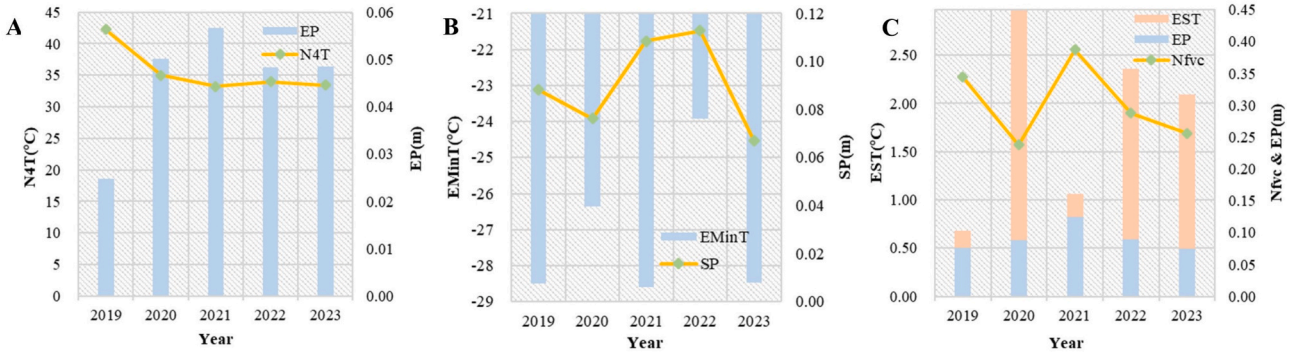

Fig. 8. Driving factors for hotspot areas and suitable habitat changes.

5. Conclusion

We established a nationwide indicator system for monitoring suitable grasshopper habitats based on the developmental mechanisms of seven dominant grasshopper species. The results identified surface and soil temperatures during the egg stage as the most influential factor in the occurrence of *Oedaleus* species. Elevation was identified as the most significant factor for *C. dubius* and *L. migratoria tibetensis*, whereas soil factors were crucial for the occurrence of *O. chinensis*. At the 99 % confidence level, grasshopper occurrence exhibited a significant spatial autocorrelation ($p < 0.01$) with the primary HAGs located in northwestern HJLK, western HL, and northeastern XW. Furthermore, a large-scale grasshopper habitat monitoring model was developed by incorporating landscape and spatial heterogeneity with adaptive weight updating. The CL-GWLR model, which integrates these factors, outperformed the models that considered omitted landscapes or spatial heterogeneity. Suitable grasshopper habitats accounted for 31–38 % of the total grassland area, with key distributions in northwestern HJLK, northern and eastern XW bordering HJLK, western HL, northern and western XJ, southwestern GSNI and XC, and northeastern QH. A comparison of the HAG results derived from point-based data with the habitat suitability monitoring results obtained from the CL-GWLR model revealed that the monitoring range of the most suitable habitats was larger than that of the HAGs. This discrepancy highlights the inherent limitations of point-based surveys, which fail to capture the full spatial extent of grasshopper habitats. Conversely, remote-sensing technology, with its ability to provide continuous spatiotemporal aerial data, offers a more comprehensive and detailed understanding of habitat suitability across larger areas. In vast grassland regions, relying solely on manual searches is inadequate for meeting the demands of precise large-scale monitoring. This study highlights the advantages of remote sensing over point-based surveys. Remote sensing provides continuous spatiotemporal aerial information, enabling more comprehensive monitoring. This methodological framework supports the eco-friendly management of grasshopper populations, providing essential guidance for sustaining grassland ecosystems and promoting the livestock industry.

CRediT authorship contribution statement

Jing Guo: Writing – review & editing, Writing – original draft, Visualization, Methodology, Investigation, Formal analysis, Data curation. **Wenjiang Huang:** Writing – review & editing, Funding acquisition, Conceptualization. **Yingying Dong:** Writing – review & editing, Methodology, Conceptualization. **Kejian Lin:** Project administration, Funding acquisition. **Fangzheng Yue:** Writing – review & editing, Resources. **Yanmin Shan:** Resources, Investigation. **Huan Liu:** Validation, Investigation. **Zhuoqing Hao:** Visualization, Supervision, Software. **Ning Wang:** Investigation, Data curation. **Xiaolong Ding:** Supervision.

Funding

This work was supported by National Key R&D Program of China (2022YFD1400500), Research on Remote Sensing Monitoring of Crop Growth and Disease and Pest under the Background of Climate Change (E44702010T), The Project of Northern Agriculture and Livestock Husbandry Technical Innovation Center, Chinese Academy of Agricultural Sciences (BFGJ2022002), GEO-PDRS: Global Vegetation Pest and Disease Dynamic Remote Sensing Monitoring and Forecasting, 2023–2025.

Declaration of competing interest

The authors declare that they have no known competing financial interests or personal relationships that could have appeared to influence the work reported in this paper.

Acknowledgments

The authors sincerely thank Xianwei Zhang for their assistance with the field survey. We also thank the academic editors and reviewers for their insightful comments, which have greatly helped us improve the quality of this manuscript.

Appendix A. Supplementary material

Supplementary data to this article can be found online at https://doi.org/10.1016/j.isprsjprs.2025.05.033.

References

Allison Jr, P.F., Lieb, D.A., Loughman, Z.J., 2022. Distribution, natural history, and conservation of cambarus dubius in Pennsylvania. J. Nat. Hist. 56 (13–16), 829–848.
Assuncao, R.M., Reis, E.A., 1999. A new proposal to adjust Moran's I for population density. Stat. Med. 18 (16), 2147–2162.
Badenhausser, I., Gouat, M., Goarant, A., Cornulier, T., Bretagnolle, V., 2012. Spatial autocorrelation in farmland grasshopper assemblages (Orthoptera: Acrididae) in Western France. Environ. Entomol. 41 (5), 1050–1061.
Bengtsson, J., Bullock, J., Egoh, B., Everson, C., Everson, T., O'connor, T., Lindborg, R., 2019. Grasslands—more important for ecosystem services than you might think. Ecosphere 10 (2), e02582.
Bhattacharjee, K., Das, S., 2022. A search for good pseudo-random number generators: Survey and empirical studies. Comp. Sci. Rev. 45, 100471.
Bidau, C.J., Mino, C.I., Castillo, E.R., Martí, D.A., 2012. Effects of abiotic factors on the geographic distribution of body size variation and chromosomal polymorphisms in two neotropical grasshopper species (Dichroplus: Melanoplinae: Acrididae). Psyche: A J. Entomol. 2012 (1), 863947.
Carlier, L., Rotar, I., Vlahova, M., Vidican, R., 2009. Importance and functions of grasslands. In: Notulae Botanicae Horti Agrobotanici Cluj-Napoca, pp. 25–30.
Chen, G., 2008. *Effects of temperature and photoperiod on the growth, development and egg diapause of three grasshopper species in Inner Mongolia* (Master). Inner Mongolia Agri. Univ. (in Chinese).
Colvin, J. (1997). Biotic and abiotic factors affecting the population dynamics of the Senegalese grasshopper, Oedaleus senegalensis . In: New Strategies in Locust Control. Birkhäuser Basel. https://doi.org/10.1007/978-3-0348-9202-5_8.
Du, B., Wei, J., Lin, K., Lu, L., Ding, X., Ye, H., Wang, N., 2022. Spatial and temporal variability of grassland grasshopper habitat suitability and its main influencing factors. Remote Sens. (Basel) 14 (16), 3910.
Fan Y., Tu. X., Hong J., Zhao L., Liu Y., Du G., Zhang Z. (2015). Biological Control of Grassland Grasshopper: Current Status and Prospects. *Grassland and livestock, 03*, 1-4 +28. (In Chinese).
García-Pérez, A., 2006. t-tests with models close to the normal distribution. Adv. Distribut. Theory, Order Stat. Inference 363–379.
Gauffre, B., Mallez, S., Chapuis, M.P., Leblois, R., Litrico, I., Delaunay, S., Badenhausser, I., 2015. Spatial heterogeneity in landscape structure influences dispersal and genetic structure: empirical evidence from a grasshopper in an agricultural landscape. Mol. Ecol. 24 (8), 1713–1728.
Geng, Y., Zhao, L., Dong, Y., Huang, W., Shi, Y., Ren, Y., Ren, B., 2020. Migratory locust habitat analysis with PB-AHP model using Time-Series satellite images. IEEE Access 8, 166813–166823.
Geng, Y., Zhao, L., Huang, W., Dong, Y., Ma, H., Guo, A., Sun, R., 2022. A landscape-based habitat suitability model (LHS model) for oriental Migratory Locust area extraction at large scales: a case study along the Middle and lower Reaches of the Yellow River. Remote Sens. (Basel) 14 (5), 1058.
Ghodousi, M., Sadeghi-Niaraki, A., Rabiee, F., et al., 2020. Spatial-temporal analysis of point distribution pattern of schools using spatial autocorrelation indices in Bojnourd city. Sustainability 12 (18), 7755.
Guo, J., Lu, L., Dong, Y., Huang, W., Zhang, B., Du, B., Huang, Y., 2023. Spatiotemporal distribution and main influencing factors of grasshopper potential habitats in two steppe types of inner mongolia, China. Remote Sens. 15 (3), 866.
Guo, J., Huang, W., Dong, Y., Lin, K., Zhou, Y., Wang, N., Zhao, F., 2024. Spatiotemporal monitoring of grasshopper habitats using multi-source data: Combined with landscape and spatial heterogeneity. *Int. J. Appl. Earth Observ. Geoinform.* 130. https://doi.org/10.1016/j.jag.2024.103838.
Guo, Z., Li, H., Gan, Y., 2006. Grasshopper (Orthoptera: Acrididae) biodiversity and grassland ecosystems. Insect Sci. 13 (3), 221–227.
Hao, S., Kang, L., 2004. Effects of temperature on the post-diapause embryonic development and the hatching time in three grasshopper species (Orth., Acrididae). J. Appl. Entomol. 128 (2), 95–101.
Hui, Z., 2013. Threshold temperature and effective accumulated temperature for oedaleus infernalis saussure. J. Shenyang Agri. Univ.
Humphreys, J.M., Srygley, R.B., Branson, D.H., 2022. Geographic variation in migratory grasshopper recruitment under projected climate change. Geographies 2 (1), 12–30.
Hu, T., Cao, M., Zhao, X., Liu, X., Liu, Z., Liu, L., Guo, Y., 2024. High-resolution mapping of grassland canopy cover in China through the integration of extensive drone imagery and satellite data. ISPRS J. Photogrammetry Remote Sens. 218, 69–83.
Huang, J., Song, L., Yu, M., et al., 2022. Quantitative spatial analysis of thermal infrared radiation temperature fields by the standard deviational ellipse method for the uniaxial loading of sandstone. Infrared Phys. Technol. 123, 104150.

Impagliazzo R, Levin L A, Luby M. Pseudo-random generation from one-way functions [C]//Proceedings of the twenty-first annual ACM symposium on Theory of computing. 1989: 12-24.

Ji, M., & Ma, X. (2015). Occurrence and Control Measures of Oxya chinensis in the Panjin Region. Northen aice, 45(01), 42+44. doi:10.16170/j.cnki.1673-6737.2015.01.016 (In Chinese).

Ji, Q., Su, L., & Chen, J. (1991). Determination and Application of the Developmental Threshold Temperature and Effective Accumulated Temperature for Overwintering Eggs of Oxya chinensis. Pest and Disease Monitoring(02), 65. (In Chinese).

Jin, C., Wu, Y., 1978. Preliminary Observations on the Biology of Chorthippus dubius. *Chin. Bull. Entomol.* 02 (47).

Kang, L., Han, X., Zhang, Z., Sun, O.J., 2007. Grassland ecosystems in China: review of current knowledge and research advancement. Philos. Trans. R. Soc., B 362 (1482), 997–1008.

Karpakakunjaram, V., Kolatkar, M.D., Muralirangan, M., 2002. Effects of abiotic factors on the population of an acridid grasshopper, Diabolocatantops pinguis (Orthoptera: Acrididae) at two sites in southern India: a three-year study. J. Orthoptera Res. 11 (1), 55–62.

Kennedy-Shaffer, L., 2019. Before p< 0.05 to beyond p< 0.05: using history to contextualize p-values and significance testing. Am. Stat. 73 (sup1), 82–90.

Kistner-Thomas, E., Kumar, S., Jech, L., Woller, D.A., 2021. Modeling rangeland grasshopper (Orthoptera: Acrididae) population density using a landscape-level predictive mapping approach. J. Econ. Entomol. 114 (4), 1557–1567.

Kühnast, C., Neuhäuser, M., 2008. A note on the use of the non-parametric Wilcoxon-Mann-Whitney test in the analysis of medical studies. GMS Ger. Med. Sci. 6, Doc02.

Latchininsky, A.V., Sivanpillai, R., 2010. Locust habitat monitoring and risk assessment using remote sensing and GIS technologies. In: *Integrated Management of Arthropod Pests and Insect Borne Diseases*. Springer, pp. 163–188.

Lecours, V., Devillers, R., Schneider, D.C., et al., 2015. Spatial scale and geographic context in benthic habitat mapping: review and future directions. Mar. Ecol. Prog. Ser. 535, 259–284.

Leksono, A.S., Yanuwiadi, B., Afandhi, A., Farhan, M., Zairina, A., 2020. The abundance and diversity of grasshopper communities in relation to elevation and land use in Malang. Indonesia. Biodiversitas J. Biolog. Diversity 21 (12).

Li, K., Li, W., Liang, K., Li, F., Qin, G., Liu, J., Li, X., 2024. Gut microorganisms of locusta migratoria in various life stages and its possible influence on cellulose digestibility. mSystems e00600–e624.

Liu, C., Feng, G., Wu, D., & Wang, J. (1997). The Study on the Starting Development and Effectively Accumnulative Temperatures in Use for the Young Locust , Chorthippus dubius (Zubovsky) Uvrov. *Sichuan Garssland*(04), 50-52+55. (In Chinese).

Loughman, Z.J., 2010. Ecology of cambarus dubius (upland burrowing crayfish) in north-central west virginia. Southeast. Nat. 9 (sp3), 217–230.

McPherson, J.M., Jetz, W., Rogers, D.J., 2006. Using coarse-grained occurrence data to predict species distributions at finer spatial resolutions—possibilities and limitations. Ecol. Model. 192 (3–4), 499–522.

Mohaymany, A.S., Shahri, M., Mirbagheri, B., 2013. GIS-based method for detecting high-crash-risk road segments using network kernel density estimation. Geo-spatial Inf. Sci. 16 (2), 113–119.

Mukerji, M., Gage, S., 1978. A model for estimating hatch and mortality of grasshopper egg populations based on soil moisture and heat. Ann. Entomol. Soc. Am. 71 (2), 183–190.

Mulkern, G.B., 1967. Food selection by grasshoppers. Annu. Rev. Entomol. 12 (1), 59–78.

Nagendra, H., Lucas, R., Honrado, J.P., et al., 2013. Remote sensing for conservation monitoring: assessing protected areas, habitat extent, habitat condition, species diversity, and threats. Ecol. Ind. 33, 45–59.

Naves, P., de Sousa, E., 2009. Threshold temperatures and degree-day estimates for development of post-dormancy larvae of Monochamus galloprovincialis (Coleoptera: Cerambycidae). J. Pest. Sci. 82, 1–6.

Neke, K.S., Du Plessis, M.A., 2004. The threat of transformation: quantifying the vulnerability of grasslands in South Africa. Conserv. Biol. 18 (2), 466–477.

Ni, S., Lockwood, J.A., Wei, Y., Jiang, J., Zha, Y., Zhang, H.J.A., 2003. Ecosystems Spatial clustering of rangeland grasshoppers (Orthoptera: Acrididae) in the Qinghai Lake region of northwestern China. Agriculture, Ecosystems 95 (1), 61–68.

Orchard, I., Loughton, B.G.A., 1980. Hypolipaemic factor from the corpus cardiacum of locusts. Nature 286 (5772), 494–496.

Piou, C., Marescot, L., 2023. Spatiotemporal risk forecasting to improve locust management. *Curr. Opin Insect. Sci.* 56, 101024. https://doi.org/10.1016/j.cois.2023.101024.

Pourghasemi, H., Moradi, H., Fatemi Aghda, S., 2013. Landslide susceptibility mapping by binary logistic regression, analytical hierarchy process, and statistical index models and assessment of their performances. Nat. Hazards 69, 749–779.

Qiu, X., Kang, L., Li, H., 2004. The economic threshold for control of the major species of grasshoppers on inner Mongolian rangeland. Acta Entomologica Sinica 05, 595–598. https://doi.org/10.16380/j.kcxb.2004.05.009.

Ren, J., Tu, X., Ge, J., Zhao, L., Zhang, Z., 2016. Influence of temperature on the development, reproduction, and life table of Calliptamus italicus (L.)(Orthoptera: Acridoidea). J. Asia Pac. Entomol. 19 (1), 203–207.

Steck, C.E., Bürgi, M., Coch, T., Duelli, P., 2007. Hotspots and richness pattern of grasshopper species in cultural landscapes. Biodiversity Conservation 16, 2075–2086.

Sun, Z., Ye, H., Huang, W., et al., 2023. Assessment on potential suitable habitats of the grasshopper Oedaleus decorus asiaticus in north China based on MaxEnt modeling and remote sensing data. Insects 14 (2), 138.

Tappan, G.G., Moore, D.G., Knausenberger, W.I., 1991. Monitoring grasshopper and locust habitats in Sahelian Africa using GIS and remote sensing technology. Int. J. Geograph. Inform. Syst. 5 (1), 123–135.

Vennard, C., Nguama, B., Dillon, H., Oouchi, H., Charnley, A., 1998. Effects of the juvenile hormone mimic pyriproxyfen on egg development, embryogenesis, larval development, and metamorphosis in the desert locust Schistocerca gregaria (Orthoptera: Acrididae). J. Econ. Entomol. 91 (1), 41–49.

Veran, S., Simpson, S.J., Sword, G.A., Deveson, E., Piry, S., Hines, J.E., Berthier, K., 2015. Modeling spatiotemporal dynamics of outbreaking species: influence of environment and migration in a locust. Ecology 96 (3), 737–748. https://doi.org/10.1890/14-0183.1.

Vierra, A., Razzaq, A., Andreadis, A., 2023. Categorical variable analyses: chi-square, Fisher exact, and mantel–haenszel. In: Translational Surgery. Academic Press, pp. 171–175.

Waldner, F., Babah Ebbe, M.A., Cressman, K., Defourny, P., 2015. Operational monitoring of the desert locust habitat with earth observation: an assessment. ISPRS Int. J. Geo Inf. 4 (4), 2379–2400.

Wang, L., Zhuo, W., Pei, Z., Tong, X., Han, W., Fang, S., 2021. Using long-term earth observation data to reveal the factors contributing to the early 2020 desert locust upsurge and the resulting vegetation loss. Remote Sens. (Basel) 13 (4), 680.

WumaErbieke, & Ling, X. (2007). Determination of Developmental Threshold Temperature and Effective Accumulated Temperature for Oedaleus decorus decorus Germar, Calliptamusitalicus, and Gomphocerussibiricussibiricus. *Livestock Industry in Xinjiang*(S1), 30-31. doi:10.16795/j.cnki.xjxmy.2007.s1.013 (In Chinese).

Xia, X., Yang, Z., Liao, Y., Cui, Y., Li, Y., 2010. Temporal variation of soil carbon stock and its controlling factors over the last two decades on the southern Song-nen Plain Heilongjiang Province. Geosci. Front. 1 (1), 125–132.

Xu, L., Yang, P., Liang, W., Liu, W., Wang, W., Luo, C., Huang, M., 2019. A radiomics approach based on support vector machine using MR images for preoperative lymph node status evaluation in intrahepatic cholangiocarcinoma. Theranostics 9 (18), 5374.

Yu, G., Shen, H., Liu, J., 2009. Impacts of climate change on historical locust outbreaks in China. J. Geophys. Res. Atmos. 114 (D18).

Zhang, G., Zhu, A.X., He, Y.C., et al., 2020. Integrating multi-source data for wildlife habitat mapping: a case study of the black-and-white snub-nosed monkey (Rhinopithecus bieti) in Yunnan, China. Ecol. Ind. 118, 106735.

Zhang, X., Huang, W., Ye, H., Lu, L., 2023. Study on the identification of habitat suitability areas for the dominant locust species Dasyhippus barbipes in inner Mongolia. Remote Sens. (Basel) 15 (6), 1718.